Available online at www.sciencedirect.com
SCIENCE DIRECT®
Surface Science 537 (2003) 241–246
SURFACE SCIENCE
www.elsevier.com/locate/susc

Fractal-compact island transition and self-limiting growth of pentacene on polymers

Yi Luo, Guanzhong Wang, James A. Theobald, Peter H. Beton *

School of Physics and Astronomy, University of Nottingham, Nottingham NG7 2RD, UK

Received 12 December 2002; accepted for publication 17 April 2003

Abstract

A mode of self-limiting growth has been identified which results in the formation of isolated monolayer and multilayer crystalline islands of pentacene with widths up to 20 μm. A size dependent transition from rough to compact monolayer island growth is observed experimentally and confirmed using numerical simulations. Nucleation of a second layer acts as a self-limiting mechanism beyond which lateral growth is suppressed and islands grow normal to the surface with the simultaneous formation of dendritic crystallites.

Keywords: Growth; Nucleation; Dendritic and/or fractile surfaces

The growth of thin films is controlled by kinetic processes such as diffusion and aggregation and may be understood within an established theoretical framework [1–3]. In the initial stages of growth, molecules diffuse until they randomly combine to nucleate a stable island. Further nucleation occurs until the characteristic separation of nucleated islands is comparable with the diffusion length of adsorbed molecules. At this point, for which the coverage may still be sub-monolayer, nucleation of new islands is suppressed and lateral growth of existing islands proceeds through the capture of diffusing molecules and continues until neighbouring islands meet. In this paper we describe a variation on this model. In particular, following the initial stages of nucleation, lateral growth is limited by the nucleation of second layers, rather than the presence of neighbouring islands. A competition between growth due to diffusive capture and the incorporation of molecules directly incident on the islands leads to a size dependent transition from a morphology with rough edges to a more compact geometry.

These effects have been observed in the growth of single crystals of pentacene (see inset to Fig. 1(a) for molecular structure), a material investigated widely for applications in molecular electronics [4–6], on polymer (poly-methyl-methacrylate (PMMA)) thin films. These substrates were chosen since they have a low density of heterogeneous nucleation sites.

A solution of 3% by weight of PMMA (ICI Acrylics) in chlorobenzene was spin coated (4000 rpm) onto pieces (6×8 mm^2) of silicon on which a 200 nm thick oxide had been grown. The PMMA

* Corresponding author. Fax: +44-115-951-5180.
E-mail address: peter.beton@nottingham.ac.uk (P.H. Beton).

0039-6028/03/$ - see front matter
doi:10.1016/S0039-6028(03)00605-8

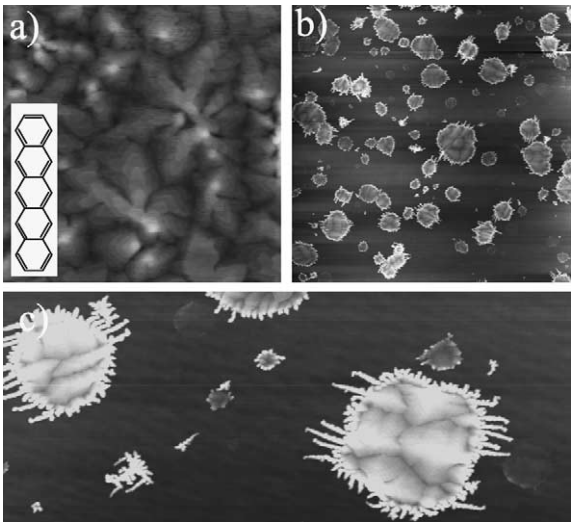

Fig. 1. AFM images of pentacene islands grown on PMMA (a) room temperature, thickness 13 nm, growth rate 2.5 nm/min, scan size 3×3 μm^2; (b) 81 °C, equivalent deposited thickness 65 nm (note sticking coefficient <1), rate 1.8 nm/min, scan size 117×117 μm^2; (c) as (b) but scan area 48.5×22 μm^2. Inset—molecular structure of pentacene.

was then baked at 180 °C for 2 h giving a film thickness ~90 nm (measured using atomic force microscopy (AFM)). Pentacene (Aldrich) was sublimed onto the PMMA coated Si/SiO_2 in a vacuum system at $\sim 10^{-6}$ Torr. A thermocouple and a quartz crystal microbalance were used to measure substrate temperature and deposition rate. Images of the sample were acquired using an AFM operating in tapping mode under ambient conditions.

For deposition at room temperature (Fig. 1(a)) we observe multilayer terraced grains with widths ~2 μm, similar to pentacene films on SiO_2 [5]. However, for substrate temperatures ~78–85 °C isolated monocrystalline islands with widths up to 20 μm are formed as shown in Fig. 1(b) and (c). The largest islands in Fig. 1(c) are multilayers and, most unusually, the thickest parts of islands (i.e. highest points in topographic AFM images) are at their edges, rather than their centres. In addition arrays of near parallel needle-like crystallites with typical widths and spacings ~200 nm grow outwards from the island edges. There is a clear correlation between needle growth and location around the island perimeter with the longest crystallites formed on two opposing island edges. The correlation of anisotropic growth on different edges indicates that the pentacene islands are crystalline. Co-existing on this surface are smaller multilayer islands, islands with heights of one or a few layers and much smaller dendritic islands.

We have investigated the influence of deposition rate, deposition time and substrate temperature on the growth mechanism. Fig. 2 shows AFM images of samples for which monolayer islands predominate. In Fig. 2(a) a large near-circular monolayer island is shown with a width ~9 μm which displays neither dendritic needle growth (Fig. 1(c)) nor fractal geometry [4]. AFM images of islands with partial second and higher layers (Fig. 2(b)) show that nucleation occurs at the edges, rather than the centres of monolayer islands. The step height for both the monolayers and higher layers $\sim 1.4 \pm 0.1$ nm (Fig. 2(c)), close to the value for polycrystalline pentacene thin films [5].

A size dependent roughness of edges is revealed from a comparison of monolayer islands having widths ranging from 0.2 to 3.5 μm (see Fig. 3 and

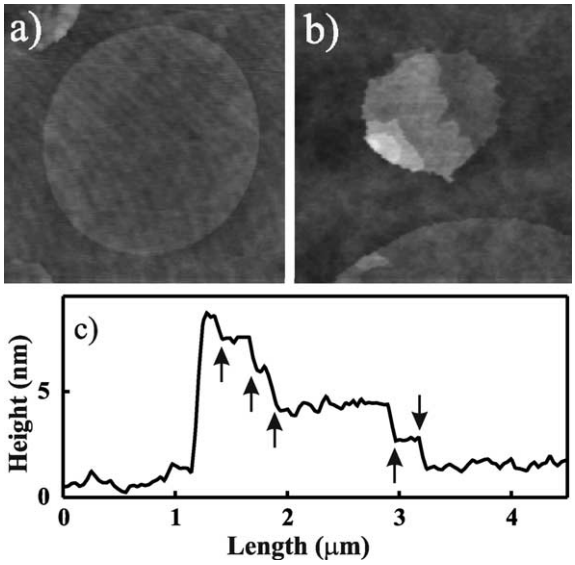

Fig. 2. AFM images of pentacene monolayer and partial multilayer islands (a) 79 °C, equivalent deposited thickness 13 nm, rate 0.75 nm/min, scan size 11×11 μm^2; (b) 83 °C, equivalent deposited thickness 20 nm, rate 1.0 nm/min, scan size 4.5×4.5 μm^2. The banding present in (a) is an imaging artefact.

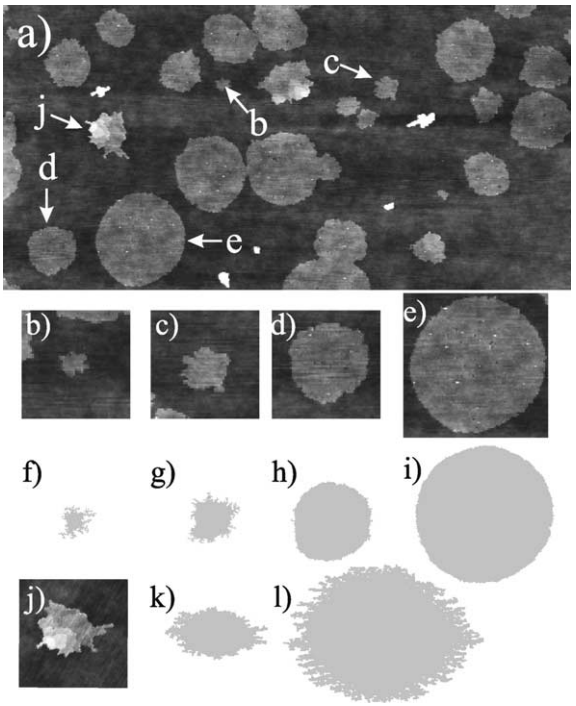

Fig. 3. AFM images of monolayer islands and simulated island shapes (a) 80 °C, equivalent deposited thickness 6.5 nm, rate 1.3 nm/min, scan area 20×10 μm^2. The figures (b)–(e), (j) are zoomed areas of islands with varying diameters as marked on (a) (2.3×2.3 μm^2 for (b)–(d), (j), 3.5×3.5 μm^2 for (e)). Islands (b)–(e) should be compared with simulated shapes calculated for $N_D = 70$, $N_T = 1000$ (f), 3000 (g), 1000 (h), 30 000 (i). Simulated island shapes for anisotropic diffusive capture with $N_D = 70$, $P = 0.2$ are shown in (k) ($N_S = 3000$, $N_T = 3500$), and (l) ($N_S = 15000$, $N_T = 21000$) show the development of anisotropic needle growth.

compare Fig. 3(b)–(e)). Clearly the largest islands have the smoothest edges. Also of note is the initial growth of the needle dendrites, *but only for islands on which higher layers have been nucleated* (Fig. 3(j)).

A comparison of Figs. 1–3 is strongly suggestive that islands initially grow laterally as monolayers, and then undergo a transition to a mode for which vertical growth occurs and the needle-like crystallites are formed. The monolayer islands thus form the base of the multilayer islands. Furthermore, a comparison of many samples shows that the width of multilayer islands is not strongly dependent on the island density. For example multilayer islands may be observed in effective isolation many tens of μm from other adsorbed material. This implies that the transition from monolayer to multilayer growth is intrinsic to individual islands, and does not depend on an effective interaction with neighbouring islands [7]. The transition must therefore be due to a *self-limiting* mechanism.

The growth of monolayer islands may be described using equations for the rate of change of N_1, the number of molecules incorporated in the monolayer island, and N_2, the number of second layer molecules on the monolayer,

$$(R \ll D_{\mathrm{cap}}) \quad \frac{\mathrm{d}N_1}{\mathrm{d}t} = F\pi D_{\mathrm{cap}}^2 + \frac{N_2}{\tau_s} f\left(\frac{L}{A}\right) \approx F\pi D_{\mathrm{cap}}^2 + FA \ \text{(steady state)}$$

$$(R \gg D_{\mathrm{cap}}) \quad \frac{\mathrm{d}N_1}{\mathrm{d}t} = 2F\pi R D_{\mathrm{cap}} + \frac{N_2}{\tau_s} f\left(\frac{L}{A}\right) \approx 2F\pi R D_{\mathrm{cap}} + FA \ \text{(steady state)}$$

$$\frac{\mathrm{d}N_2}{\mathrm{d}t} = FA - \frac{N_2}{\tau_s} f\left(\frac{L}{A}\right)$$

where A, L and R are the island area, perimeter and radius, F is the incident molecular flux and τ_s^{-1} is the rate at which molecules at the island edge hop over the Ehrlich–Schwoebel barrier [8]. The function $f(L/A)$ is the probability that a second layer molecule occupies an edge site. It is assumed that: (i) no second layer molecules are desorbed (corresponding physically to a high sticking coefficient for pentacene on pentacene—confirmed by post annealing up to ~130 °C which results in no changes in either individual islands or the general morphology); (ii) D_{cap} characterises the length scale over which the island acts as a sink for molecules incident on PMMA; (iii) no second layer nucleation has occurred; (iv) the rate of upward jumps of molecules from the edge of the first layer to the second layer is negligibly small. The last point is valid since pentacene is a layered material [4–6] and so the adsorption energy of an individual molecule will be much greater at the edge, as opposed to on top, of an existing monolayer. This accounts for the formation of the large two-dimensional monolayers shown in Fig. 2. In quasi-steady state $\mathrm{d}N_2/\mathrm{d}t \approx 0$ and the equations for $\mathrm{d}N_1/\mathrm{d}t$ reduced to the simplified form shown above.

At room temperature the diffusion length is sufficiently long that the inequality $R \ll D_{cap}$ is always satisfied. Monolayer growth is dominated by capture of molecules diffusing on PMMA and continues until neighbouring islands meet. This results in morphologies such as Fig. 1(a). Since $D_{cap} \propto \exp[(E_A - E_B)/2kT]$ (E_A and E_B are respectively the desorption and diffusion barriers for pentacene [1–3]) the above inequality may break down at elevated substrate temperature. A reduction in D_{cap} occurs for temperatures $\geqslant 78$ °C, as confirmed by a reduction in the effective sticking coefficient of pentacene by $\sim 10^3$ over the range 78–85 °C (measured for a deposition rate of 0.8 nm/min).

Our results for monolayer growth are consistent with a value for D_{cap} which satisfies the inequality $R \ll D_{cap}$ during the initial stages of growth, followed by a size dependent transition beyond which $R \gg D_{cap}$. In these two regimes growth is dominated by, respectively: (i) diffusive capture of molecules which were originally incident on PMMA; (ii) molecules which impinge directly on the island, diffuse to the edges, hop over the Ehrlich–Schwoebel barrier and become incorporated in the growing monolayer (see Fig. 4 upper inset). The growth rates for these processes are proportional to island radius and area respectively. Lateral growth of *large* monolayer-high islands is thus dominated by directly impinging molecules and continues until a second pentacene layer is nucleated. A partially formed second layer acts as a sink for second layer molecules thus inhibiting further lateral growth and triggering a transition to vertical growth through the formation of higher layers.

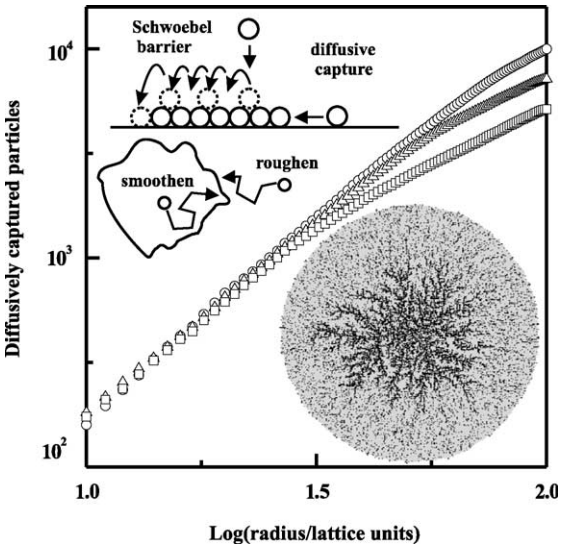

Fig. 4. Lower inset—simulated island ($N_D = 200$, $N_T = 70000$) in which diffusively captured molecules are black, those from direct impingement are in grey highlighting initial fractal growth as confirmed by plot of number of particles within a circle versus circle radius for $N_D = 50$ (□), 100 (△), 200 (○). For small radius the plot is linear with slope 1.83 ± 0.03. Upper inset—schematic diagrams illustrating the growth process.

Growth through diffusive capture (dominant for small islands) leads to roughened (fractal [9]) edges, while that due to direct impingement (dominant for large islands) acts to smoothen edges resulting in compact islands. The size-dependent competition between roughening and smoothening (see Fig. 4 inset) accounts for the variation in edge roughness observed in Fig. 3 for large and small islands. This mechanism for a rough-smooth transition is intrinsic to individual islands, rather than a result of interactions between neighbouring islands as previously considered [3,7].

A numerical model, a variation of the diffusion limited aggregation model DLA [10], confirms this model of monolayer growth. A seed molecule is positioned at the origin of a square grid. Further molecules are then randomly placed with co-ordinates (x, y) and allowed to diffuse by randomly incrementing or decrementing their x or y co-ordinate by 1. Molecules impinging on unoccupied sites (PMMA) diffuse and, if they visit a site adjacent to an occupied site, are frozen at this position and added to the growing monolayer. However if such molecules diffuse through N_D hops they are removed (desorbed) from the simulation and a new molecule added. Molecules impinging on occupied sites (pentacene monolayer) diffuse until they reach the island edge and are then transferred into an adjacent vacant site (hopping over the Ehrlich–Schwoebel barrier). Molecules which impinge on top of the growing island can diffuse through an unlimited number of hops—they are never desorbed.

Simulated island shapes for $N_D = 70$ are shown in Fig. 3(f)–(i) (for a total number $N_T = 1000$,

3000, 10 000 and 30 000 molecules) in which occupied sites are shown in grey. There is a striking agreement between the size dependent evolution of the simulated shape and the observed size dependence in zoomed AFM images (Fig. 3(b)–(e)). Note that edge diffusion, which is omitted from our simulations, leads to additional smoothing of the very fine fractal growth around the edges of small islands which is observed in our simulations, but not our experiments [11].

The fractal nature of the simulated results and the transition to compact growth is emphasised in Fig. 4 inset in which diffusively captured molecules are shown in black and those incorporated following direct impingement are in grey. The fractal (black) network due to diffusive capture during initial growth is present for small radii. At larger radii, where growth due to direct impingement dominates, there is a near random incorporation of diffusively captured (black) molecules. These islands have been analysed by plotting the number of diffusively captured molecules within in a circle versus circle radius on a log–log scale (Fig. 4) for several values of N_D. For small radii the curves follow a common straight line with a non-integral gradient 1.83 ± 0.03, confirming the fractal geometry of this model of growth. The change in gradient at larger radius (see Fig. 4) signals a transition to compact growth. As expected this transition occurs at larger radii for larger values of N_D.

Nucleation of a second layer of pentacene provides an alternative sink for molecules directly incident on the island. This inhibits the incorporation of such molecules in the first layer and thus suppresses the competition between smoothing and roughening. Further lateral growth is due to diffusive capture only. The diffusive capture of molecules at the edge of a near circular island results in the nucleation of dendrites which accounts for the formation of the needle-like crystallites shown in Figs. 1 and 3. This is confirmed by simulations in which capture of molecules incident on the island is switched off after the island has accumulated N_S molecules, following which diffusive capture continues until a total N_T molecules are incorporated. The comparison with experiment is complicated by crystalline anisotropy which is included in the simulations by ascribing a probability, P, for diffusive capture of molecules forming a bond in the y-direction [12]. Simulated islands (Fig. 3(k) and (l) with parameters $N_D = 70$, $P = 0.2$) show the formation of dendrites and have shapes comparable to Figs. 3(j) and 1(c) providing support for our model. The small dendrites (bottom left, Fig. 1(c)) are presumed to grow from islands on which second layer nucleation occurs at the very early stages of monolayer growth.

Second layer nucleation has been studied extensively [13,14], although nucleation at island edges (see Figs. 2 and 3), is inconsistent with existing theoretical models [13]. Presumably microscopic processes, as yet unknown, lead to an increased residence time, equivalent to reduced diffusivity, at the island edge. In addition the fractal-compact transition results in a non-trivial perimeter/area ratio so that the dependence of second layer nucleation rate on island size is extremely complex. However, for large near-circular islands with random occupation of edge sites $(f(L/A) \propto L/A)$ the second layer nucleation rate, K_2, reduces to $K_2 \propto R^i$ (i is the minimum number of molecules required to nucleate a stable island).

We have identified a size-dependent transition from fractal to compact island geometry. A simple physical model generates islands which undergo a transition from rough (similar to DLA) to smooth (similar to Eden model [9]) edges. The transition combines with a self-limiting process to result in large organic crystals on polymeric substrates which are relevant to molecular electronics.

Acknowledgements

This work was supported by the UK Engineering and Physical Sciences Research Council and the University of Nottingham. We are grateful for helpful discussions with Dr. P. Moriarty, Dr. C.J. Mellor and Dr. M. Swift.

References

[1] J.A. Venables, Surf. Sci. 299/300 (1994) 798.
[2] H. Brune, Surf. Sci. Rep. 31 (1998) 121.
[3] J.G. Amar, F. Family, P.-M. Lam, Phys. Rev. B 50 (1994) 8781.

[4] F.-J. Meyer zu Heringdorf, M.C. Reuter, R.M. Tromp, Nature 412 (2001) 517.
[5] S.F. Nelson, Y.-Y. Lin, D.J. Gundlach, T.N. Jackson, Appl. Phys. Lett. 72 (1998) 1854.
[6] C.D. Dimitrakopoulos, I. Kymissis, S. Purushothaman, D.A. Neumayer, P.R. Duncombe, R.B. Laibowitz, Adv. Mater. 11 (1999) 1372;
C.D. Dimitrakopoulos, S. Purushothaman, I. Kymissis, A. Callegair, J.M. Shaw, Science 283 (1999) 822.
[7] G.S. Bales, D.C. Chrzan, Phys. Rev. Lett. 74 (1995) 4879.
[8] G. Ehrlich, F.G. Hudda, J. Chem. Phys. 44 (1966) 1039;
R.L. Schwoebel, J. Appl. Phys. 40 (1968) 614.
[9] See A-L. Barbarasi, H.E. Stanley (Eds.), Fractal Concepts in Surface Growth, Cambridge University Press, Cambridge, 1995, and references therein.
[10] T.A. Witten Jr., L.M. Sander, Phys. Rev. Lett. 47 (1981) 1400.
[11] Z. Zhang, X. Chen, M.G. Lagally, Phys. Rev. Lett. 73 (1994) 1829.
[12] R.C. Ball, R.M. Brady, G. Rossi, B.R. Thompson, Phys. Rev. Lett. 55 (1985) 1406.
[13] J. Tersoff, A.W. Denier van der Gon, R.M. Tromp, Phys. Rev. Lett. 72 (1994) 266.
[14] J. Rottler, P. Maass, Phys. Rev. Lett. 83 (1999) 3490.